POLITECNICO DI TORINO

Master in Materials Engineering

Synthesis of multi-cationic dawsonite, towards a versatile high-entropy oxide synthesis route

Supervisors:

Prof. Matteo Pavese (Polito)

Prof. Michael Stuer (Empa)

Candidate:

Pietro Allegri

Academic Year 2021-2022

Serial number: 288622

Summary

0. Abstract

High-entropy materials are known in metallurgy for a long time but only since 2015, they have emerged in the ceramic community gathering more and more interest due to their interesting properties. These promising materials are composed of no less than five cations that could lead to surprising catalytic properties and more. The interesting properties arise thanks to a single-phase stabilization due to the configurational entropy; furthermore high-entropy ceramics are typically semiconductors or insulators with the presence of a band gap that makes them potential functional materials. Due to the combination of cations with different valences, we obtain a material with surprising catalytic properties due to a so-called *"charge distortion"*. This phenomenon is due to the uneven electron cloud distribution between the metals with different valences and the oxygen. This phenomenon may improve the catalytic performances of the material. These oxides could be useful for CO_2 reduction or H_2S removal [3] [4] [5]. This is the reason why they are now at the centre of a growing field considering the global energetic crisis, and the lack of precious metals. The goal of this thesis is to start with a short description of high-entropy ceramics and the origin of their behaviour, after that moving to the synthesis of a new type of high-entropy hydroxide and its characterization. The centre of the work is the synthesis of a five-cations high-entropy ceramic, a new precursor of a high-entropy oxide, called *Dawsonite.* In addition, another path through this material is described following a solid-state synthesis for achieving the same high entropy mixture. On the side, there is the development of a new type of segmented flow reactor completely automatized for high throughput synthesis of new high-entropy ceramics. The importance of this device is related to the capacity of changing the proportions between the constituents. These areas are the two main topics of the work and starting point for the next developments in research concerning the catalytic activities of these ceramics.

1. Introduction

1.1 High entropy Materials

The concept of high entropy ceramics is inherited from the field of high entropy alloys (HEAs). In general, can be delineated the parameters responsible for setting of a high-entropy alloy:

1. The enthalpy of mixing and the configurational entropy are related to the potential of the HEAs formation. High enthalpy implies segregation or clustering. On the other hand, if we consider the entropy effect, increasing the number of cations increases the entropy stabilization of the structure [3]. These two parameters are determining for the mixing as well.
2. The valence of the cations and the coordination, which means the size of the cations, should be appropriate for the lattice structure. At the same time, the cations valence should maintain the charge balance [3].

If we look at two-components alloy (AB), the entropy stabilization can be explained if we consider that a single phase will form only when mixing leads to a reduction of the Gibbs free energy according to equation 1.

$$\Delta G_{mix} = \Delta H_{mix} - T \cdot \Delta S_{mix}$$

Equation 1: Gibbs free energy expression.

Where ΔG_{mix} is the difference of free Gibbs energy (J/mol) between the initial and the final state of the mixing, ΔH_{mix} is the enthalpy of mixing and ΔS_{mix} is the entropy of mixing. In general (also in a multiphase systems) when the mixing entropy increases, the Gibbs free energy decreases, and the solid solution becomes more stable. Since we are looking at a two-phase alloy the addends above can be written down as equations 2 and 3.

$$\Delta S_{mix} = -R \cdot (x_A \ln x_A + x_B \ln x_B)$$

Equation 2: Entropy of mixing.

$$\Delta H_{mix} = ZN \cdot \left(E_{AB} - \frac{E_{AA} + E_{BB}}{2}\right) x_A x_B$$

Equation 3: Enthalpy of mixing.

where E_{AB}, E_{AA}, E_{BB} are the bond energies between atoms, Z is the coordination number, N is the Avogadro number, X_A, X_B is the mole fractions of A and B respectively and R is the universal gas constant [6].

When $\Delta H_{mix} < 0$ and $\Delta H_{mix} = 0$ (ideal solution) the Gibbs energy becomes negative, favouring the formation of a single phase [6]. However, in case $\Delta H_{mix} > 0$, due to differences in atomic size or electronegativity, the entropic term ($-T\Delta S_{mix}$) must be high enough in order to overcome ΔH_{mix} and stabilize the solid solution ($\Delta G_{mix} < 0$) [7].

In general, the entropy of mixing involves two major contributions, the vibrational entropy ΔS_{vib}, related to the distribution of energy states in the crystal and the configurational entropy ΔS_{conf}, related to the distribution of atoms in the lattice sites. Now we assume that the maximization of entropy of mixing means to maximize only the configurational entropy and neglect vibrational entropy. We obtain the result shown below in figure 1.

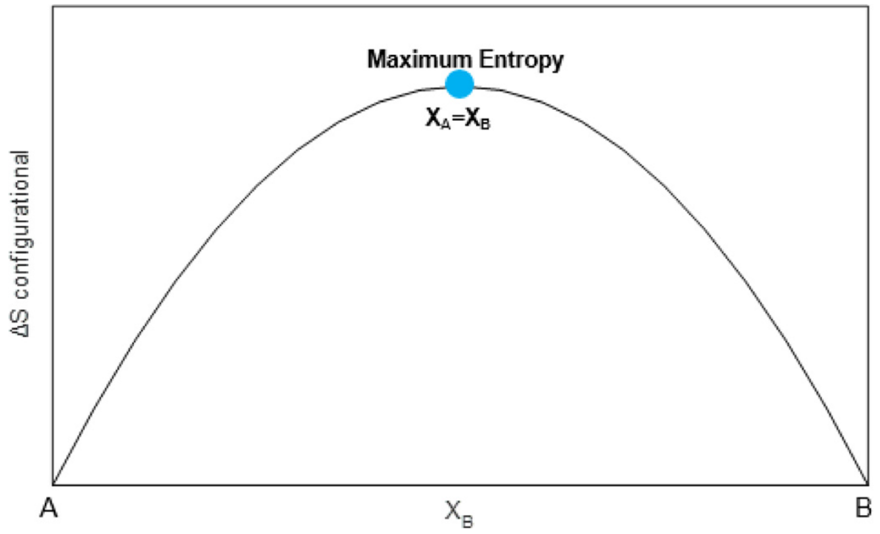

Figure 1: Distribution of configurational entropy [3].

When the quantities of the two components of the alloy are the same (equimolar) it is reached a maximum in configurational entropy that leads to a decrease of the Gibbs free energy enabling the stability and the monophasic structure of the alloy [3] [6]. For this binary system this means that is obtained $X_A=X_B$. In addition, the maximum of the configurational entropy scales with the number of components as shown in figure 2.

This is the principle of HEA's they exhibit high entropy of mixing to overcome the positive enthalpy of mixing value.

1.2 High entropy Oxides

In HEO's the reasoning is a bit more complicated. The presence of the oxygen in the lattice interferes and breaks the first neighbour interactions of the atoms in the cation sublattice [4]. This effect is registered for all the cations that are surrounding by the oxygen. This leads to $\Delta H_{mix}=0$ and leaves only the entropic term so that the free Gibbs energy of mixing is regulated only by the configurational entropy ($\Delta G_{mix}= -T\Delta S_{mix}$). This is the principle of entropy-stabilized oxides (ESO).

This clarification is important because even though high-entropy and entropy-stabilization are often used interchangeably, they are fundamentally different. The concept of high entropy reflects that the system simply has high configurational entropy without any consideration to the endothermicity or exothermicity of the system. However, entropy stabilization indicates that the system needs to possess both high configurational entropy and positive enthalpy of formation (+ΔH) which means that the entropy drives the thermodynamic state of stability.

For HEO's is all true what said before on HEA's but must be considered the composition dependence of configurational entropy, because it is no more two-components alloy but is a complex system (oxide). The effect of the components on the configurational entropy is shown in equation 4.

$$S = -k_B \sum_{i=1}^{N} x_i \, ln(x_i)$$

Equation 4: Relationship between the number of components and the entropy factor.

Where X_i is the fraction of the cation i, k_b is the Boltzmann constant and N is the number of constituents.

Therefore, entropy is influenced by the number of elements and the atomic fraction of each element in the composition. Based on this equation, the entropy of mixing for a specified number of elements reaches a maximum value when the number of elements is high, and they have an equal atomic fraction as shown in figure 2. Furthermore, using equimolar amounts maximizes the configurational entropy leading to an overcome of the Gibbs free energy of formation. This aspect balances the positive enthalpic factor, where the disorder of the oxygen is assumed zero.

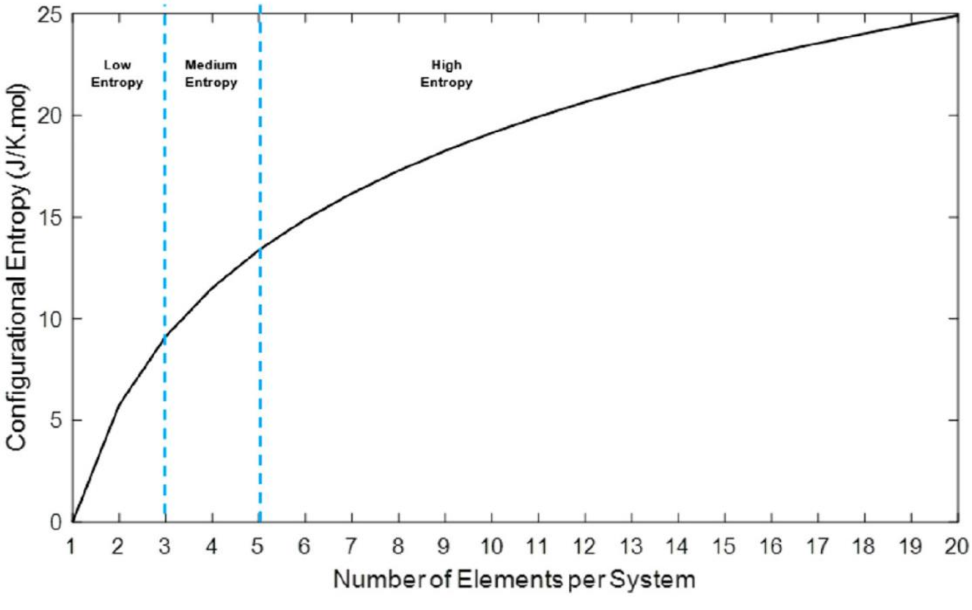

Figure 2: Relation between number of elements and entropy [3].

The comparison between metal-oxides (HEO) and alloys (HEA), based on the concepts of alloys, reveals outstanding properties of the counterpart oxides. To further understand the concept of entropy acting as a driving force, let's assume a binary metallic system described in the previous paragraph. The interaction energy between the atoms will be given by the following equation: $E_{A-B}=(E_{A-A}+E_{B-B})/2$ where the enthalpy change of mixing is zero and therefore all the atoms are contributing to the solution equally while being driven by the maximum entropy. On the other hand, the structure of metal-oxides is featured by having oxygen anions that are surrounding the cations by a specific coordination number, therefore there is no direct interaction between any two adjacent cations since they are separated by anion layers. In this case, all the cations are considered to contribute to the lattice equally, therefore, by recalling the basic thermodynamics concepts, the whole system will be driven to its maximum entropy.

Another aspect related to entropy is that it rules the change (endothermic and reversible) from a multiphase to a single-phase state. If we reduce the configurational entropy, the system tends toward a multiphase state, and the transition temperature necessary to obtain a single-phase increases [8]. Consequently, in some compositions, a phase separation at low temperatures can be recovered with annealing at high temperatures.

In conclusion observing the reasonings above we can surely say that a common definition of high-entropy ceramics is still debated but most of the literature agrees to identify such a material as an inorganic lattice containing five or more equimolar distinct cations the number of required cations however being dependant on the crystal structure [1] [2]. This formulation promotes a new kind of material that is thermodynamically stabilized by the influence of the entropic factor on free Gibbs energy. Right away are reported the known structures (figure 3).

Structure	Crystallography	Appearance
High-Entropy Oxide (HEOs)		
Rock-salt	Cubic (*Fm-3 m*)	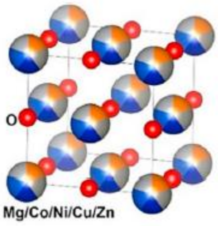
Fluorite	$A_2B_2O_7$ cubic (*Fm-3 m*)	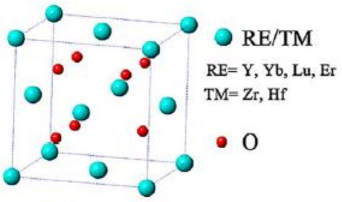
Perovskite	ABO_3 Orthorhombic (*Pbnm*)	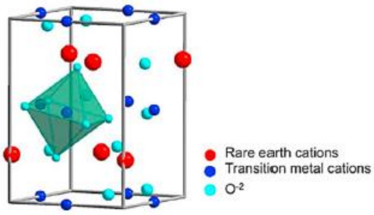
Perovskite	ABO_3 Cubic (*Pm3 m*)	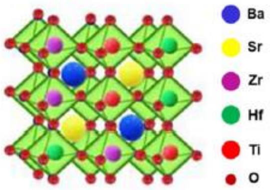

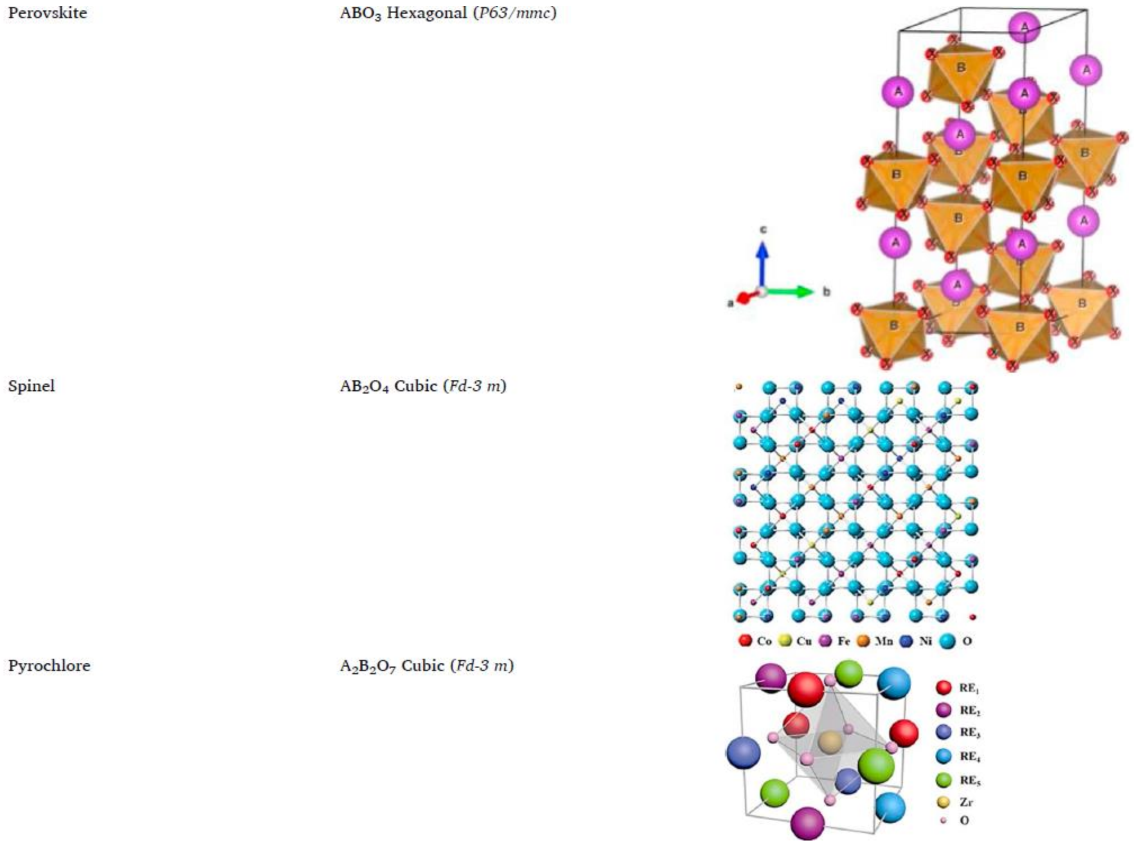

Perovskite	ABO_3 Hexagonal (*P63/mmc*)	
Spinel	AB_2O_4 Cubic (*Fd-3 m*)	
Pyrochlore	$A_2B_2O_7$ Cubic (*Fd-3 m*)	

Figure 3: Main crystal structures of HEO [2].

1.3 Applications Outlook

Over the last decade, HECs have gained increasing interest because of the wide range of potential application fields, some of which will be described in the following. This interest is driven by potential performance jumps from HECs compared to their low-entropy counterparts.

Catalysis

One of the most promising application fields of HEOs is found in catalysis. Catalysis is one of the most important and intricate processes used in the chemical industry. Finding novel catalysts with high activity and selectivity, good stability, long lifetime, as well as low cost, is the continuous pursuit of scientific researchers. In the hunt for better catalysts, many problems are encountered, such as the high cost of precious metals commonly used in catalytically active sites, the light absorption and lifetime of semiconductor photocatalytic materials, and the poisoning of catalytic active sites. Generally, catalytic processes are thermodynamically favoured, when the activity of the catalysers increases, reducing the energy required to activate the reaction (lower than the activation energy barrier ΔE). Here, HEOs are of particular interest, since from a dynamics perspective, activity and selectivity can be enhanced by chemical composition, spatial distribution, lattice distortion (which provides more active sites and intermediates), and sluggish diffusion that can contribute to the high stability of the material. Moreover, the cost can of course be controlled by element design, as shown in figure 4. [13]

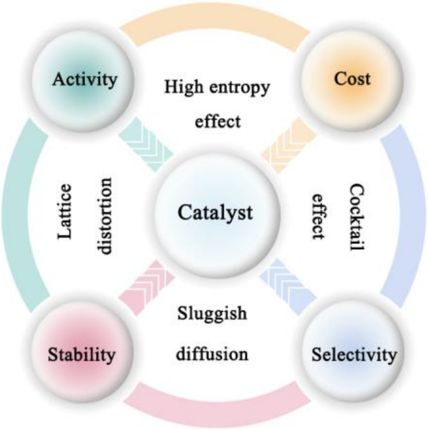

Figure 4: High entropy effect on catalysis.

Thermal protection and insulation

HEOs exhibit low thermal conductivity and excellent thermal stability. In general, thermal conductivity at low temperatures is due to the directional movement of phonons [14]. Therefore, thermal conduction is driven by various phonon-scattering processes, including phonon-phonon scattering, grain boundary scattering, and defect scattering [13]. The phonon scattering can be particularly well engineered in HEOs due to the possibility to introduce huge differences in atomic mass, ionic radius, and interatomic force between the elements that increase phonon scattering.

Batteries

Due to the high entropy and also symmetry driven by HEO such as (Mg,Co,Ni,Cu,Zn)O these materials expose high thermochemical stability that suppresses the structural deformation and the defects formation. For this reason, they have the property to maintain the performances under charge cycling [15]. This led to investigations of the suitability of high-entropy ceramics for use as anodes, cathodes and solid-state electrolytes in Li-ion batteries.

2. Dawsonite an overview

Dawsonite or usually called AACH (aluminium ammonium carbonate hydroxide) is a mineral found in nature as the product of the decomposition of aluminium silicates and feldspars. It can be included in the family of carbonate hydrates, and in naturally occurring variants holds in the crystal structure only two cations (Na and Al), thus resulting in the chemical formula: **$NaAl(CO_3)(OH)_2$**. Its crystals have usually a radial acicular structure. The crystal system properties are summarized in table 2, in addition, the structure can be seen in figures 5 and 6 [16].

CRYSTAL PROPERTIES	
Most common crystallographic system	*Orthorhombic*
Crystalline group	*Trimetric*
Symmetry	*Dipyramidal*
Lattice parameters	*a = 6,73* *b = 10,36* *c = 5,575*
Punctual group	*2/m 2/m 2/m*

Table 2: Crystal properties of Dawsonite.

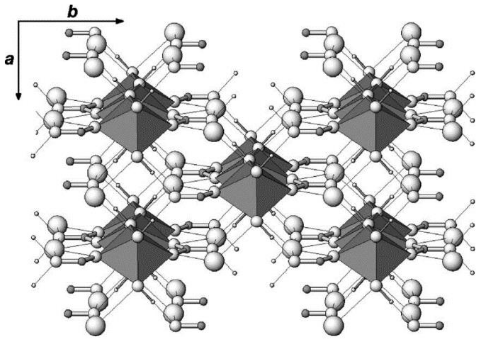

Figure 3: Dawsonite structure seen across c axis.

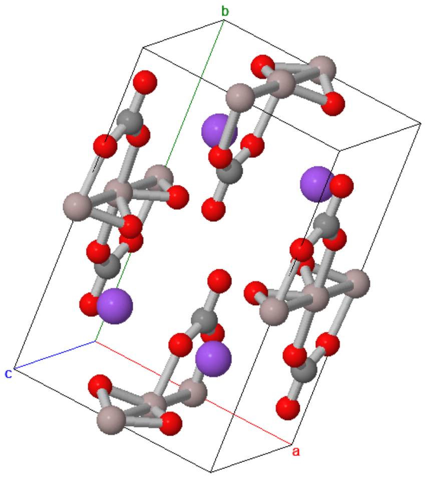

Figure 6: Crystal structure of Dawsonite [21].

Dawsonite applications are mostly found in CO_2 capture either in its natural form or by substituting one of its natural cations [17]. The capture is realized during the synthesis when the pressure of CO_2 is increased enabling more incorporation of it inside the final structure through HCO_3^-. Furthermore, this dawsonite can also serve as a precursor for oxides tailored for catalytic applications [18], as a precursor of alumina as well or when combined to hydrotalcite can form a spinel structure [16].

3. Materials and Methods

3.1 Wet Synthesis

Co-precipitation has been chosen as the wet synthesis method in the present study [19]. This choice has been driven considering it allows obtaining high purity homogeneous particles and is compatible with low reaction temperatures required for compatibility with the segmented flow reactor described below. Especially in combination with the segmented flow reactor, it offers the potential to narrow the particle size distribution and control the morphology of the final powder. The precipitation method can be synthesised with the chemical reaction:

$$CO_2 + 3\ H_2O + Al^{3+} + Fe^{3+} + Cr^{3+} + Ga^{3+} + In^{3+} \text{--->} (Al_{0.2}\,Cr_{0.2}\,Fe_{0.2}\,Ga_{0.2}\,In_{0.2})\ CO_3(OH)_2 + 4H^+$$

used during the synthesis trials.

The synthesis starts from solid precursors, in this case, we use nitrates hydrates, as shown in Table 3. We mix the desired amount of precursors with ultrapure de-ionized water (obtained using Barnstead™ MicroPure™ Water Purification System) until we obtain a homogeneous solution. The mixing has been done with magnetic stirrers in closed bottles to avoid contamination. Additionally, we mix an ammonia solution with ammonium bicarbonate and water, and we obtain a second solution. We pour the second solution into the precursor solution while stirring and we start the slow precipitation of nanopowders. The stirring reaches 1000 rpm and the pouring is almost 1 drop per second. For ensuring the maximum amount of precipitate we let stir for 20 h at 50 ˚C to guarantee the synthesis goes to completion. We obtain a brown suspension we need to separate from the solution, and we can do this with a centrifuge and then dry the powder in the oven for 6 h at 120 ˚C.

3.1.1 Chemicals

The selection of appropriate cations is crucial to successfully be able to synthesize phase pure and crystalline dawsonite. We started looking investigating cations with +3 charge, by following a literature search and noticing they were the most prominently used for the synthesis of high-entropy materials. To prevent incorporation issues, we used cations with similar ionic radius, especially avoiding bigger ones compared to Al^{3+}, primarily found in natural Dawsonite, that could be difficult to incorporate into the crystal structure. From the list of candidate cations, only those available in nitrate form were shortlisted, following the precipitation reaction requirements to start from nitrates. Following this initial shortlist, the selection of cations was further refined following incorporation trials to finally be reduced to Al^{3+}, Fe^{3+}, Cr^{3+}, Ga^{3+}, and In^{3+}.

PRECURSORS	*MOLAR MASS (g/mol)*	*PURITY (from Sigma Aldrich)*
Aluminium (III) Nitrate Nonahydrate $(Al(NO_3)_3) \cdot 9H_2O$	375,13	99,997 %
Iron (III) Nitrate Nonahydrate $(Fe(NO_3)_3) \cdot 9H_2O$	404,00	99,95 %
Chromium (III) Nitrate Nonahydrate $(Cr(NO_3)_3) \cdot 9H_2O$	400,15	99 %
Gallium (III) Nitrate Hydrate $(Ga(NO_3)_3) \cdot xH_2O$	255,74 *	99,9 %
Indium (III) Nitrate Hydrate $(In(NO_3)_3) \cdot xH_2O$	300,83 *	99,99 %

** This molar mass is calculated for anhydrous compound, since was not known the percentage of water in the precursor.*

Table 3: List of precursors.

Due to the hydrophilic nature of the nitrates, the weights of nitrates had to be in the next step optimized to yield equimolar Dawsonite powders. A few dozens of experiments were carried out to optimize the ratio among the five different salts used in the synthesis. The main issues were related to the indium and gallium salts, that are hygroscopic and whose quantity must be carefully regulated to guarantee equimolarity in the final compound. To reach this goal, thermogravimetric analysis was also carried out on Ga-nitrate and In-nitrate to roughly measure the water content. The weight reduction of In-nitrate due to water elimination at 400 °C was 60% while in the case of Ga-nitrate was around 65%. By using these values and further optimizing the ratio of the different salts it was at length possible to obtain a product with nearly 1:1:1:1:1 ratio among the five cations.

Table 4-5 below shows summarizes the final quantities required. The ammonia solution is needed to regulate the pH in order to facilitate the precipitation of the Dawsonite.

Solution 1	
Cations	**Optimized mass (g)**
$(Al(NO_3)_3) \cdot 9H_2O$	0,84
$(Fe(NO_3)_3) \cdot 9H_2O$	0,90
$(Cr(NO_3)_3) \cdot 9H_2O$	0,90
$(Ga(NO_3)_3) \cdot xH_2O$	1,15
$(In(NO_3)_3) \cdot xH_2O$	1,15
H_2O	50

Table 4: Optimized quantities of the precursor solution.

Solution 2	
Bases	**Optimized mass (g)**
Ammonia Solution 25%	10,51
Ammonium Bicarbonate	6,75
H_2O	100

Table 5: Optimized quantities of ammonia solution.

The results of this synthesis are shown more in depth in chapter 4.

3.1.2 Segmented flow reactor

Given the difficulties related to the modelling of complex oxide systems, many research efforts on HEOs are to date done experimentally, requiring high-throughput methods for efficient progress. Accordingly, the concept of segmented tubular flow reactors has been developed further, to automatically be able to screen many compositional changes in an automated way. Let's briefly have a look at the following image, the fundamental characteristics of the developed reactor will be illustrated.

First of all, we have a reservoir of all the different precursor nitrate solutions that are in different bottles (*stock solutions*). In addition, in one bottle is stored the second reactant (*solution 2)* and in a last bottle, there is a non-miscible liquid such as *dodecane*. The running force of the flow is peristaltic pumps (*Ismatec 4408*) that draw from the precursor's solutions the desired proper quantity of each and from the solution 2 bottle the corresponding amount as required for the proper amount according to the reaction described in the previous paragraph. The two solutions are injected separately in two pipes, alternatively with dodecane, coming from the continuous pump. The two flows continue moving in the tubes until they reach a switch (*Asia reactor injector*) coming from the continuous pump (*Syrris Asia syringe pump*) that enable the mixing of each of the bubbles from the solution 2 in every bubbles of the precursors, maintaining the separated by dodecane and avoiding the pulsed flow. This result is reached thanks to the work between the continuous pump and the switch. The pump connected to the switch injects the liquid coming from the two pipes in the switch, that is timed precisely puts together the two flows avoiding the mismatch of the bubbles. The result is a flow of alternate bubbles of reactants and dodecane, the main goal is to obtain the best mixing inside the bubbles as small reactors, the dodecane is just a non-polar separating liquid that ensures the separation of the bubbles reactors. Once the dodecane is injected the flow moves through the pipe in 50 ˚C water (heated by *Julabo DYNEO DD*) that moves more the equilibrium to the products. The residence time is settled for achieving the complete precipitation reaction. In the end, the tube moves into a cooling system and to a final switch that separates the dodecane from the reacted solution. That is later centrifugated. This device's scheme is shown completely in figure 7 and it must be highlighted that all the pumps, the heater and the switch are controlled by a single LabVIEW program. The program can regulate the flow of the peristaltic pump so that is possible to change the ratios of the stock solutions according to the trial we are doing at that moment.

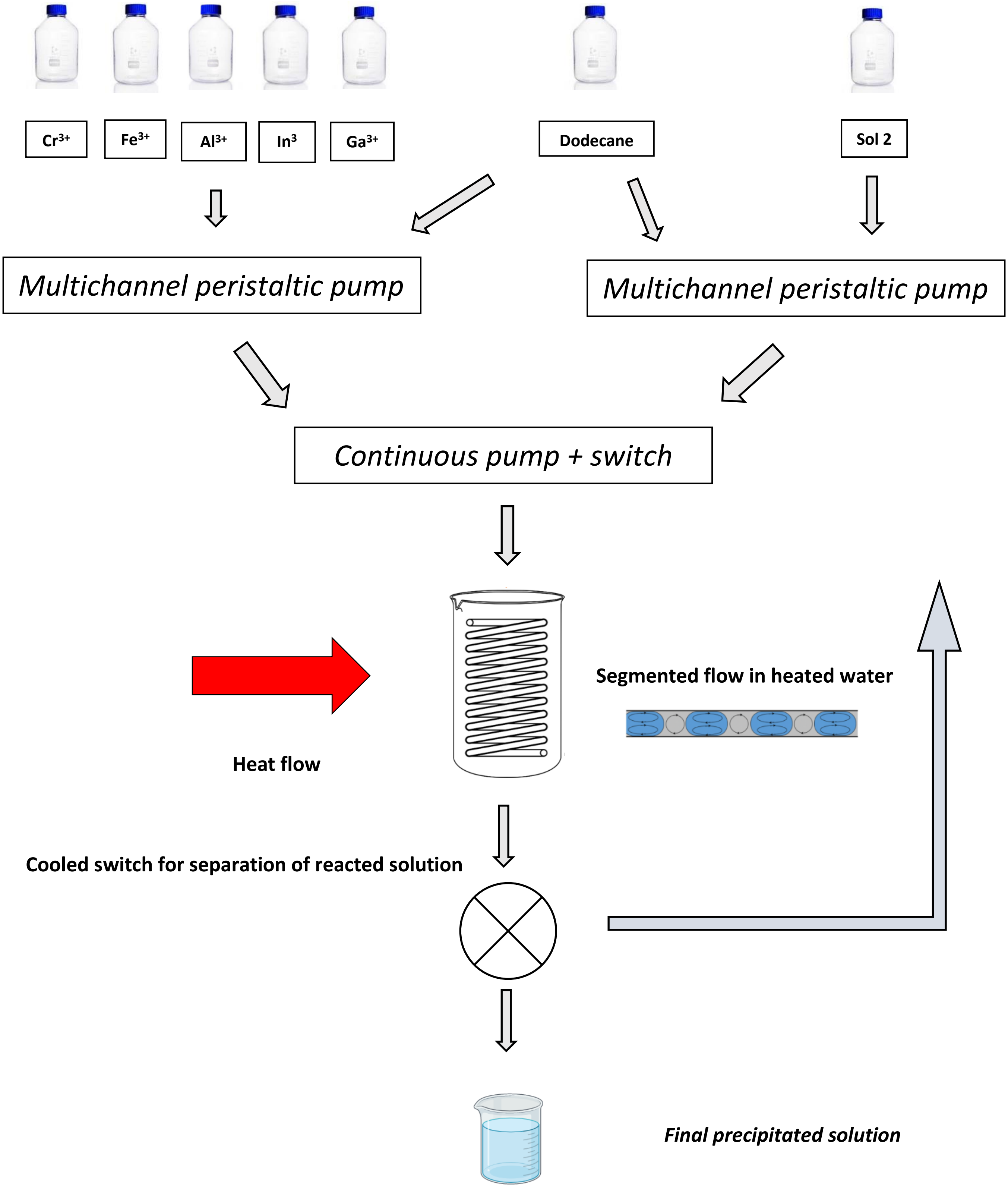

The continuous pump is necessary for achieving a continuous flow that the peristaltic pumps do not allow. The reaction starts as far as the two solutions are put in contact just before the tubular reactor, so in the end, we are able to obtain a dispersion of powder in a solution that is separated from the dodecane.

3.2 Solid State synthesis

As described earlier the Dawsonite structure may also serve as a precursor for a high-entropy oxides synthesis after appropriate heat treatment. In many cases, however, it requires the appropriate heat treatment profile and atmosphere to be identified, to ensure that this transformation, if it exists, can occur at a given cationic composition. For this very reason, to understand the behaviour of dawsonite at high temperatures and confirm the existence of the high-entropy oxide phase with the corresponding composition, solid-state synthesis was additionally performed directly using the corresponding oxides as precursors.

The oxides are weighted ensuring equimolarity, they are milled in a planetary mill with α-Al_2O_3 balls in isopropanol. After 4 hours of milling the slurry is removed and dried at 100 ˚C in air. During the milling process, we are sure we reach an equal size distribution, useful for grain growth (sintering). After that, we put the powder in the oven at four different temperatures: 800, 1000, 1200 and 1400 ° C, this sintering process is for enabling the grain growth and diffusion through the grain borders and is necessary to achieve one of the proper oxide's structures mentioned in chapter 1.

3.2.1 Powders

The powders are oxides of the five main cations, in Tables 6 and 7 we can see the correct proportions between the oxides and the molar mass of the precursors.

Cations	***Optimized mass (g)***
Al^{3+}	0,30
Fe^{3+}	0,47
Cr^{3+}	0,45
Ga^{3+}	0,56
In^{3+}	0,83

Table 6: Final mass quantities of the powder mixture.

PRECURSORS	***MOLAR MASS (g/mol)***
Aluminium Oxide (Al_2O_3)	101,96
Iron Oxide (Fe_2O_3)	159,69
Chromium Oxide (Cr_2O_3)	151,98
Gallium Oxide (Ga_2O_3)	187,84
Indium Oxide (In_2O_3)	277,64

Table 7: Molar mass quantities of HEO precursors.

4. Characterization

4.1 Dawsonite

The structure we have obtained is a five-cations dawsonite, **$(Al_{0.2}\,Cr_{0.2}\,Fe_{0.2}\,Ga_{0.2}\,In_{0.2})CO_3(OH)_2$**. It is a new high entropy material never reported before in literature. Previous synthesis studies on dawsonite focused on the incorporation of only one or two cations rather than number of cations relevant to high-entropy materials. Since there is no literature on this new material, it deserves to be characterized.

4.1.1 X-Ray Diffraction

X-Ray Diffractometry (XRD) is commonly used for studies of solid-state symmetries (atomic and molecular). In particular, it is useful for determining the crystal structure of an unknown material and is based on the interaction between an incident X-ray beam and the lattice. Since the wavelength of an X-Ray is similar to the distance between atoms, diffraction is observed. Due to Bragg's law ($n\,\lambda = 2\,d\,\sin\vartheta$) the outcoming wavelength of the beam is depending on the distance between the atomic planes (d). Since the X-Ray interacts elastically with the atoms the beam is re-emitted and creates constructive and destructive interference depending on the symmetry (as shown in figure 5). The detector catches the constructive interference at certain angles (2ϑ), so a graph is obtained with specific peaks for each material representing the direction where the beam comes from with the highest intensity. These peaks are specific for each lattice structure and cell parameters.

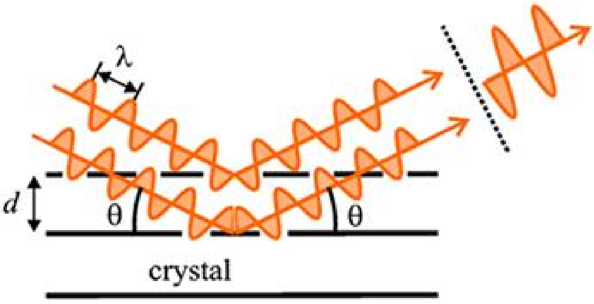

Figure 5: Interaction between the X-Ray beam and the crystal.

Here are reported the results of the X-ray diffractometry for the five cations Dawsonite obtained from the precipitation synthesis. On the *x*-axis the vertical lines correspond to the peaks of the natural Na-Al Dawsonite, however other materials in the Dawsonite family are present in the XRD database and present peaks similar to those observed in the case under study. Due to this similarity, we think it is reasonable to preliminarily assign all the peaks observed in the XRD pattern to a phase of the Dawsonite family. It is obvious that when mixing five different cations inside the crystalline structure of the Dawsonite, the XRD pattern must change, and a complete Rietveld analysis will be probably needed in the future to assess the correspondence of this pattern to the desired phase.

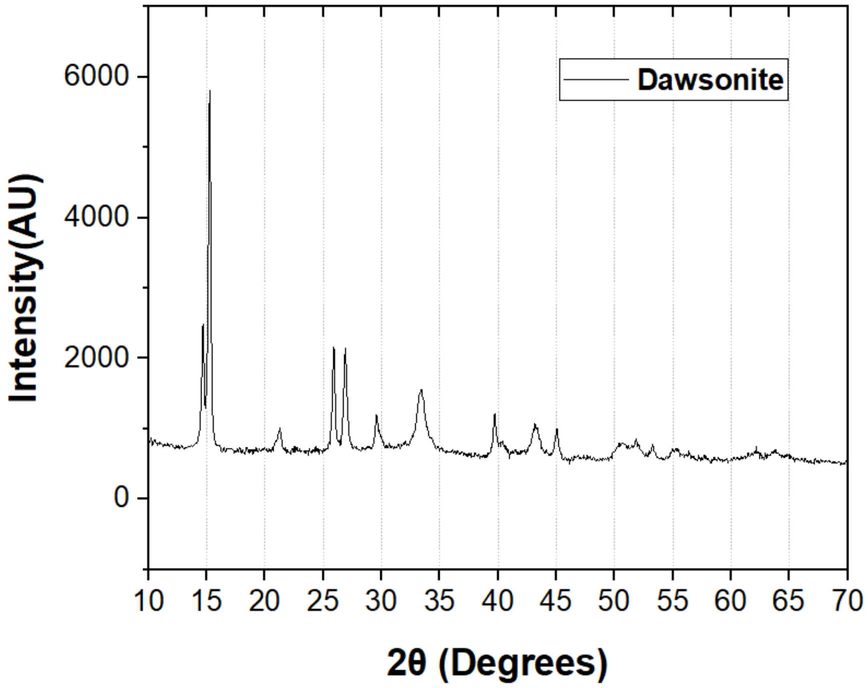

Figure 6: XRD pattern of five cations Dawsonite.

4.1.2 Scanning Electron Microscopy

Generally, this analysis is used for describing the morphology of particles, their size, eventual agglomeration and presence of different surface geometries. Successively, are reported the results of a preliminary SEM analysis. The device used was a SEM *"VEGA 3"* from *Tescan* (Czech Republic) and the software "VegaTC" has been used for the investigation of the powders. The principle of this analysis is bombarding the sample with electrons at a certain energy, the result is the extraction of secondary electrons due to the inelastic interaction between the incident electrons and the atoms of the sample. The secondary electrons come from the first layers of the sample and give us information on the morphology of the surface.

The particle is quite homogeneous. The size after a hand milling is about 5 µm, the surface appears clear from emerging crystals but with a significant agglomeration after the synthesis.

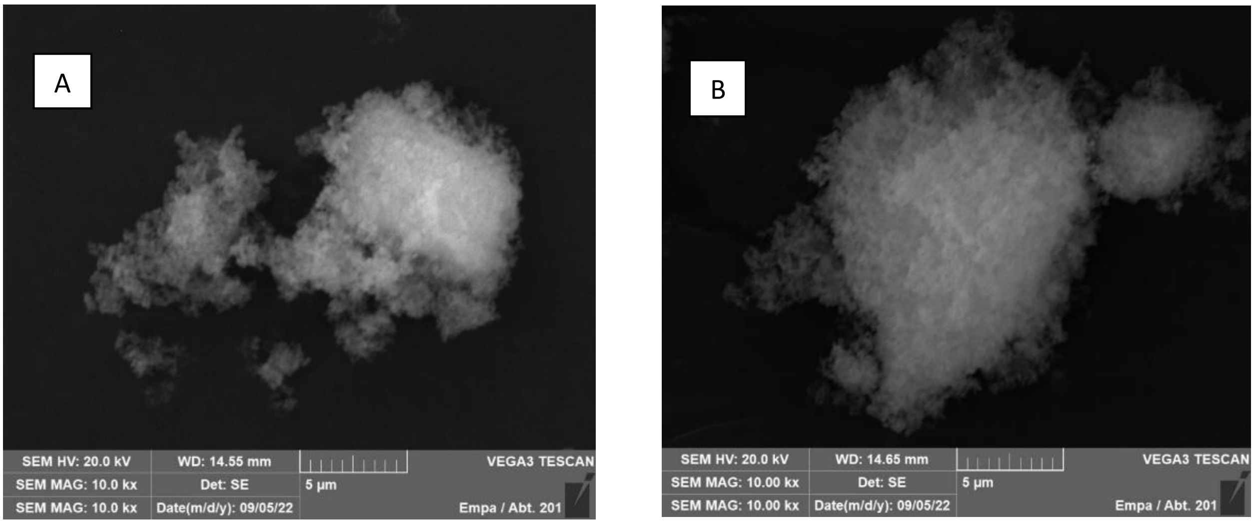

Figure 7: (A)(B) Agglomeration of nanosized particles of Dawsonite at SEM.

4.1.3 Energy Dispersive Spectroscopy

This analysis is commonly used for determining the chemical composition of an unknown material and also the distribution of the elements in the material structure. The electron beam (generated from a filament) is focused on the sample at a certain energy. The interaction between the beam and the atoms generates the expulsion of electrons from the K and L levels, and the rearrangement of the remaining electrons leads to an X-Ray emission at a certain energy or an Auger event. The EDS machine was linked to the SEM and the analysis was performed with the "XFlash 6|10" from *Bruker* (USA) detector and analysed with the software "ESPRIT 2", furthermore has been used a voltage of 20 keV.

The EDS has been the last step for controlling the synthesis, this analysis tells us the atomic percentage of the elements present in the final powder. As shown in chapter 1, equimolarity is a fundamental requirement for starting the catalytic properties of the material.

The final powder shows roughly the same amount of each cation (as shown in table 8), according to the experimental error due to the machine, which is known as ± 1,5 % due to the calibration, and to experimental errors, for instance due to the weighing process.

Cations	***Atomic percentage (%)***
Al^{3+}	20,3
Fe^{3+}	18,1
Cr^{3+}	19,1
Ga^{3+}	18,7
In^{3+}	23,8

Table 8: Atomic percentage of cations in five cations Dawsonite.

Furthermore, the distribution of the cations inside the grain is fundamental for maximizing the entropy of the substance, we must obtain cations as isotropically distributed as possible. Below are reported compositional maps of the Dawsonite obtained with the precipitation method.

The Dawsonite shows a rather homogeneous distribution of the five elements and according to the previous data also the same amount, as shown in figure 8. No secondary phases containing only one cation are observed.

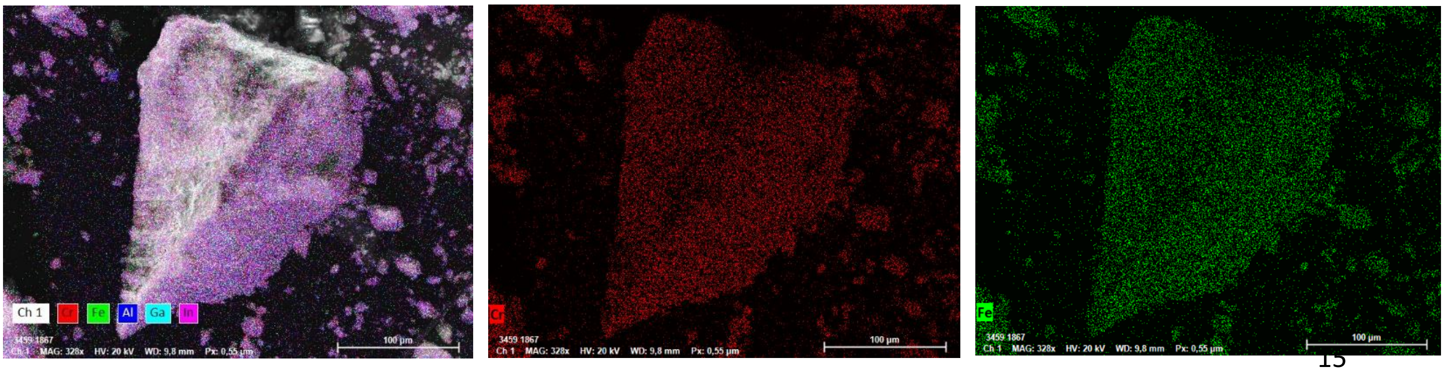

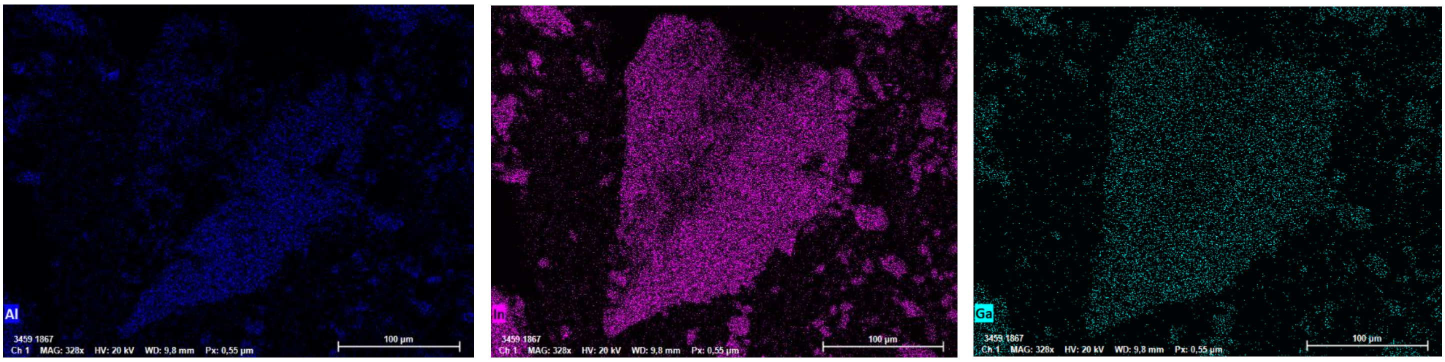

Figure 8: Distribution of five cations in Dawsonite obtained from precipitation method.

4.1.4 Thermo-Gravimetric Analysis

Commonly TGA is used for the evaluation of a generic weight loss that could be due to degradation or other phenomena. This technique is based on heating the sample to a certain temperature with a fixed heating rate in the air. The sample is held in a crucible where is constantly weighted, registering the weight loss due to the rise in temperature. The heating rate has been fixed at 10 ˚C/min and the maximum temperature achieved has been 600 ˚C.

This analysis has been done for the characterization of the water content due to chemical incorporation. As shown in figure 9, the loss of weight is around 40 % of the total mass.

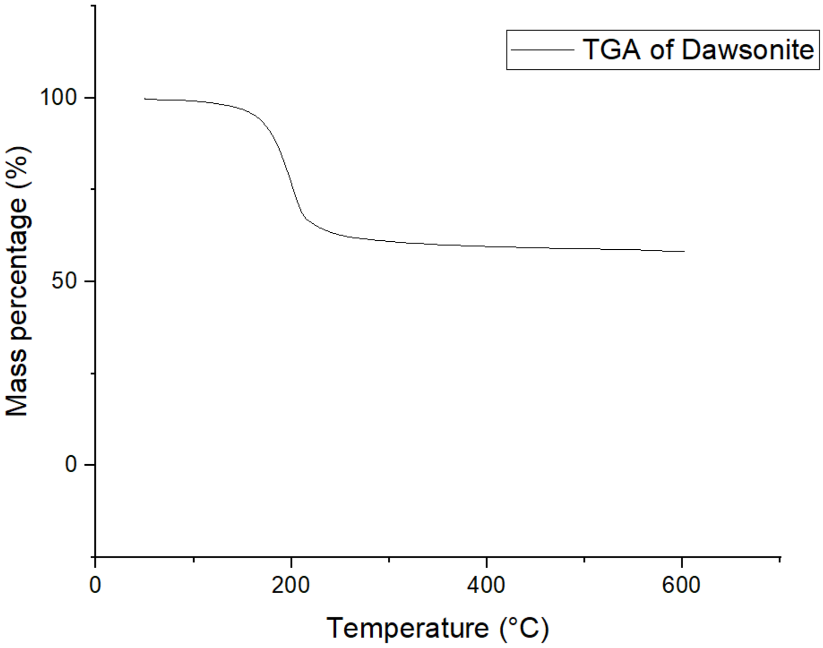

Figure 9: TGA on a five cations Dawsonite.

This result is reasonable if we assume that by heating up to 600 ˚C we turn the carbonate structure into an oxide structure like Me_2O_3. If we look at the chemical formula of the Dawsonite the percentage of OH (water) is approximately 21 %, and the percentage of CO_3^{2-} is about 39 %. If we assume that the crystallization water is completely removed and remains the oxygen, due to the oxide, we calculate a loss of 21% of water and 8% of oxygen, which leads to a mass loss of 29 %. The missing 10 % of water may represent the physisorbed water that has not been evaluated.

4.1.5 Nitrogen Adsorption

This analysis is the principal method for determining the specific surface of a material. The powder sample is put under vacuum and then slowly nitrogen (N_2), is added in order to allow its condensation inside the pores and the adsorption on the surface of the material. The measure of the volume of nitrogen adsorbed at the different partial pressures determines the volume sorbed on the surface and condensed into the pores. By using the Brunauer-Emmett-Teller (BET) model it is possible to calculate the specific surface of the material from the first part of the curve.

The investigation is necessary to quantify the surface area because of the interest in the catalytic properties of Dawsonite. A catalyst must expose as much surface as possible being in contact with the reactants of the catalytic reaction. In figure 10 and 11 are shown the results of this analysis.

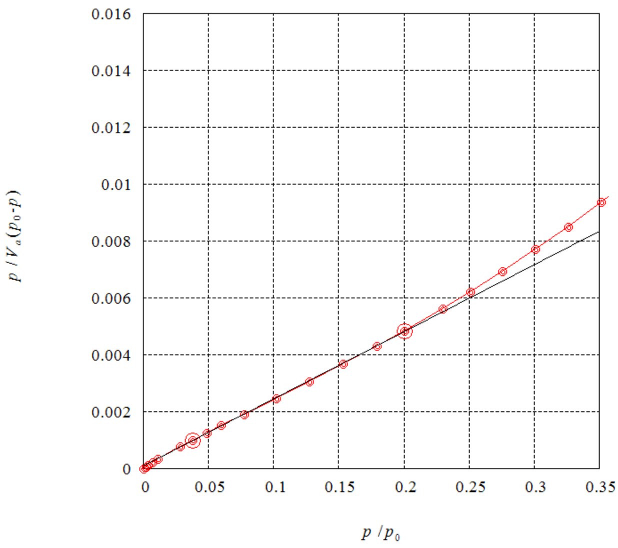

Figure 10: BET plot of Dawsonite in N_2 atmosphere.

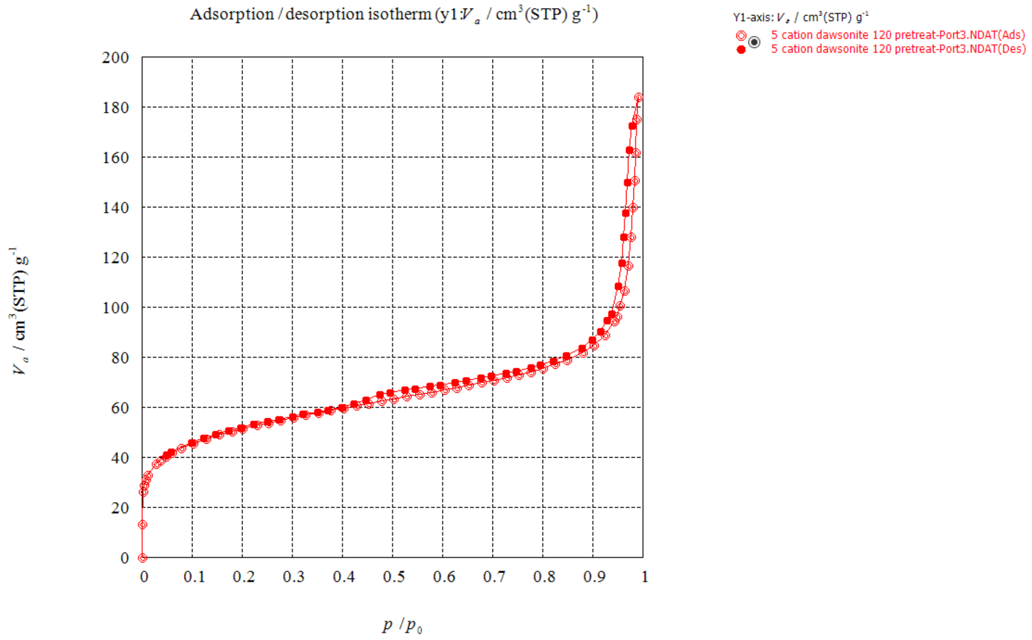

Figure 11: Isotherm of Adsorption and Desorption of Dawsonite in N_2 atmosphere.

From the first graph (Figure 10) can be extracted the specific surface equal to 1,84 · 10^2 m^2/g and the total pore volume that is about 0,2838 cm^3/g with an average pore diameter of 6,16 nm.

Furthermore, the isotherm in Figure 11 shows the typical behaviour of an isotherm type II, this curve is typical for macroporous materials. A specific surface of about 200 m^2 is considered a good result, in general a material with such a high surface is considered a “medium surface” material.

4.2 Solid state Sesquioxide

From the solid-state synthesis described in chapter three has been obtained a powder that has been put in the oven for sintering at 4 different temperatures. The final goal was to obtain an α structure of an oxide with the form of Me_2O_3, where Me represents the five cations used previously in Dawsonite.

4.2.1 X-Ray Diffraction

The XRD analysis has been done also for the results of the solid-state synthesis. Here we can see the comparison between the XRD results of the solid-state synthesis and the XRD patterns of the precursors (oxides).

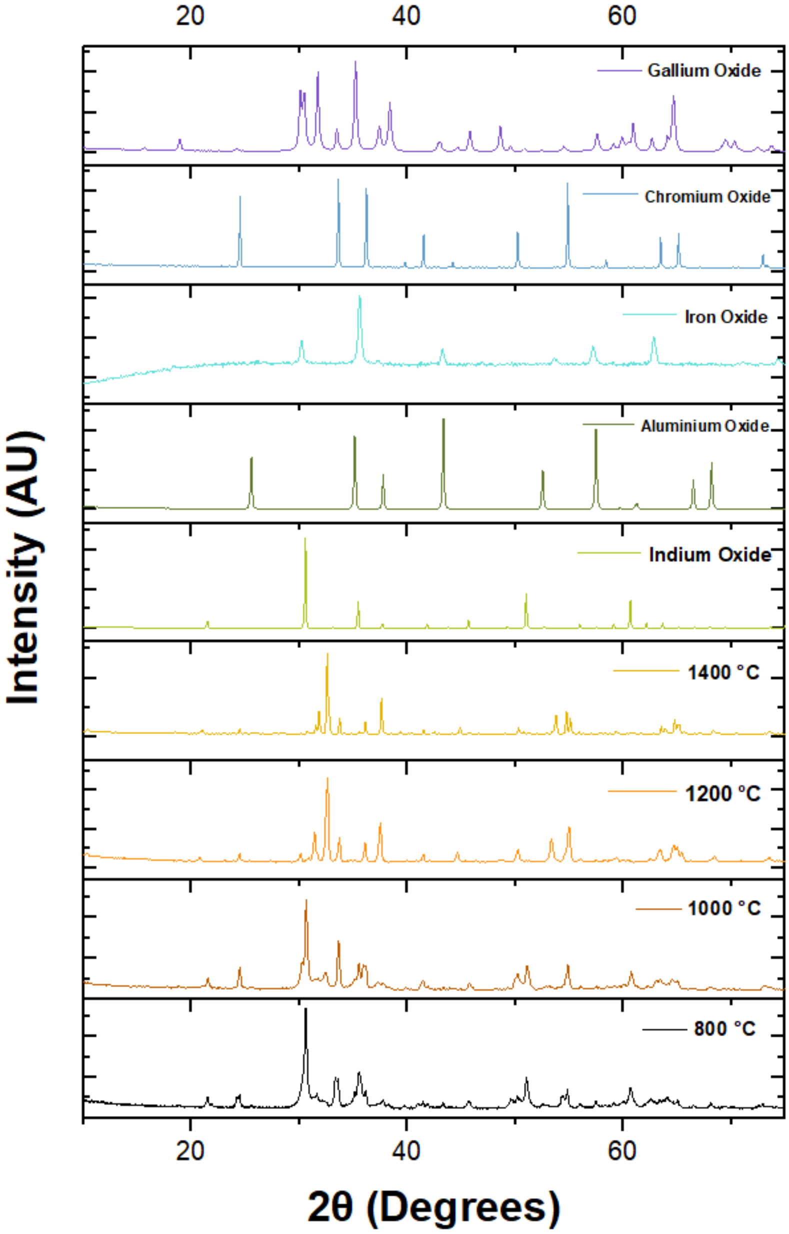

Figure 12: Comparison between solid-state products baked at different temperatures and oxides precursors.

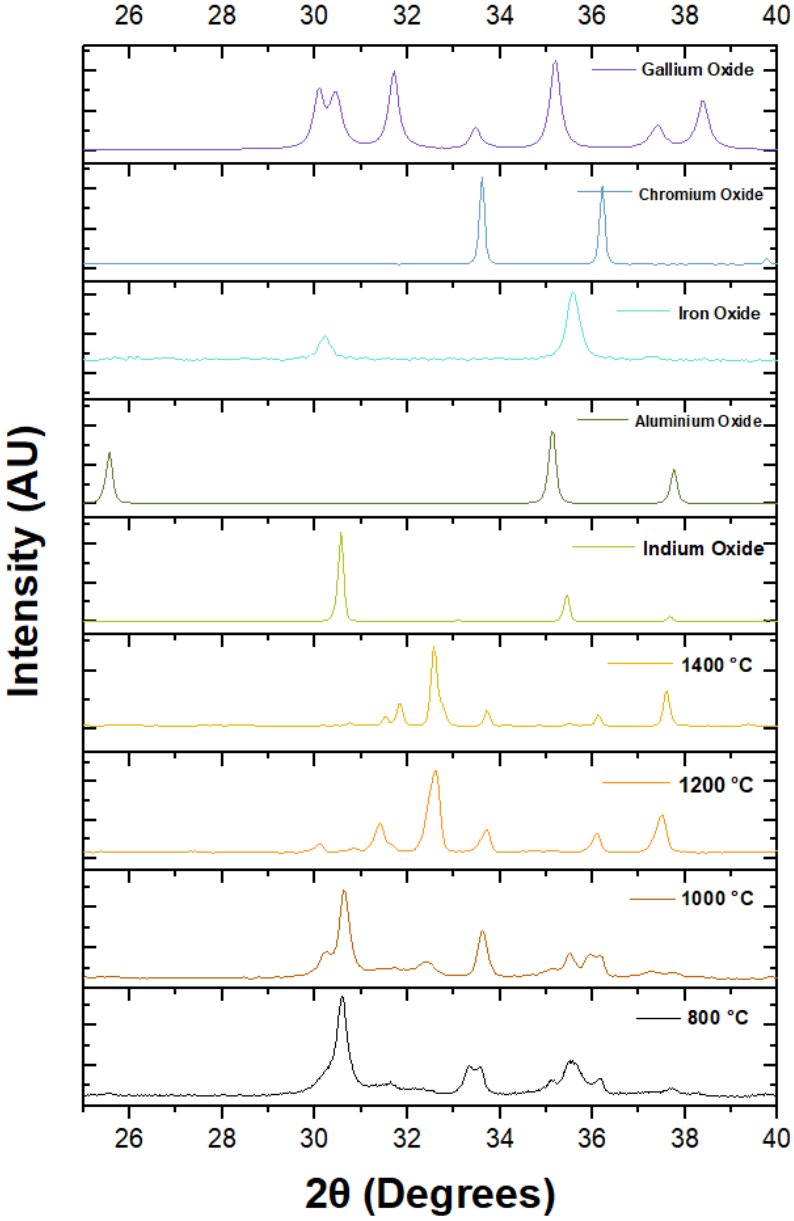

After heat treatment at 800 °C and 1000 °C some of the precursor oxides are still visible in the XRD pattern. For instance, indium oxide and chromium oxide can be observed from 21 to 25 2-theta, with 2 sharp peaks. Furthermore, the main peak could be an overlapping of indium oxide and gallium oxide around 31, and the presence of iron oxide is seen around 35. Aluminium oxide peaks are still present but very low.

According to the result of this analysis, the pattern completely changes between 1000 ˚C and 1200 ˚C, since it disappears the peak around 31 and 35, with the appearing of a peak around 37-38. This change highlights that at a temperature between 1000 ˚C and 1200 ˚C the crystal structure turns into another one that can be noticed at 1400 ˚C as well and has not been studied yet. The diffraction pattern is not similar to the one of α-Al_2O_3 or α-Cr_2O_3, however it is evident that a reaction occurred, however further studies will be needed to fully understand the phases development during the heat treatment.

5. Conclusions

The research question settled at the beginning of this six-month research was *"Can we make a new High-Entropy material with novel interesting properties for catalytic activity?"* The work performed led to the development of Dawsonite, now completely characterized.

Concerning Dawsonite, the analysis showed that this powder satisfies all requirements discussed in the first paragraph for being classified as a high-entropy material. It is probably a monophase material with homogenous dispersion of equimolar cations. However, the properties of this new material have not been studied yet.

The solid-state synthesis did not reach the final goal, to prove that exists an oxide structure with these five cations in the form of Me_2O_3. The last step to do is finding the right temperature for turning the Dawsonite structure into one of the typical HEO structures.

The reactor will be useful for the synthesis of different materials with different compositions and properties in a completely automatized way, saving time and being efficient as an important resource of Empa's laboratories.

In the end, the most important result has been the synthesis of a new high-entropy material never discovered before, this material can represent an encouraging substance that can be studied or used as a precursor for research in the high entropy ceramic field.

6. References

[1] A. A. G. N. H. K. P. Shaima H. Albedwawi, «High entropy oxides-exploring a paradigm of promising catalysts: a review,» *Materials & Design,* pp. 1-27, 29 January 2021.

[2] K. P. a. A. M. Efstathiou, «Effects of Sol−Gel Synthesis on 5Fe−15Mn−40Zn−40Ti−O Mixed Oxide Structure and its H2S Removal Efficiency from Industrial Gas Streams,» *Environmental Science & Technology,* pp. 4367-4372, 12 May 2009.

[3] O. Y. O. Erdogan Alper, «CO2 utilization: Developments in conversion processes,» *Petroleum,* pp. 109-126, 26 November 2016.

[4] K. E. E. K. E. E. David A. Porter, Phase Transformations in Metals and Alloys, Boca Raton: CRC Press, 2009.

[5] J. Y. .. P. B. B.S. Murty, High-Entropy Alloys, Elsevier, 2019.

[6] E. S. T. B. A. M. E. D. D. H. J. S. C. a. J. M. C.M. Rost, «Entropy-stabilized Oxides,» *Nature communications,* 2015.

[7] C. T. S. C. Corey Oses, «High-entropy ceramics,» 2020.

[8] E. S. T. B. A. M. E. D. D. H. J. J. S. C.M. Rost, «Entropy-stabilized oxides,» *Nature Communications,* 2015.

[9] P. E. M. F. K. E. Saeid Akrami, «High-entropy ceramics: Review of principles, production and applications,» *Materials Science & Engineering R,* vol. 146, 7 October 2021.

[10] Y. X. F.-z. D. H. W. L. S. L. M. G. Z. Y. W. X. Q. L. Y. H. W. B. Z. J. L. Y. Z. Huimin XIANG, «High-entropy ceramics: Present status, challenges, and a look forward,» *Journal of Advanced Ceramics,* vol. 10, n. 3, pp. 385-441, 2021.

[11] M. J. R. Rui-Zhi Zhang, «Review of high entropy ceramics: design, synthesis, structure and properties.,» *Journal of Materials Chemistry A,* 20 September 2019.

[12] C. O. M. E. D. H. G. N. K. C. M. R. D. W. B. J. M. a. S. C. Cormac Toher, «High-entropy ceramics: Propelling applications through disorder,» *MRS BULLETIN ,* vol. 47, 2022.

[13] D. Barthelmy, «Webmineral,» 1997-2014. [Online]. Available: http://www.webmineral.com/crystal/Orthorhombic-Dipyramidal.shtml. [Consultato il giorno 6 9 2022].

[14] M. H. S. M. a. J. P.-R. O. Martin, «Design of hydrothermally-stable dawsonite-based sorbents in technical form for CO2 capture,» *Energy & Environmental Science,* 4 August 2014.

[15] M. A. H. M. I. Z. A. Ali, «Dawsonite-Type Precursors for Catalytic Al, Cr, and Fe Oxides: Synthesis and Characterization,» *Chemistry of Materials,* vol. 17, p. 26, November 2005.

[16] M. L. B.-N. K. Y. L. S. K. Sangwoo Nam, «Morphology controlled Co-precipitation methos for nano structured transparent MgAl2O4,» *Ceramics International,* pp. 153352-15359, 12 August 2017.

[17] E. S. T. B. A. M. E. C. D. D. H. J. L. J. S. C. &. J.-P. M. Christina M. Rost, «Entropy-stabilized oxides,» *Nature communications 6,* 29 September 2015.

[18] A. S. R. K. B. E. R. A. B. H. W. a. H. H. Ralf Witte, «High-entropy oxides: An emerging prospect for magnetic rare-earth transition metal perovskites,» *Physical Review Materials 3,* 13 March 2019.

[19] W.-M. Z.-B. J. Q.-Q. S.-K. S. Y. Y. K. P. H.-T. Yan Zhang, «Dense high-entropy boride ceramics with ultra-high hardness,» *Scripta Materialia,* vol. 164, pp. 135-139, 2019.

[20] Y. Y. H. Y. M. Z. S. M. J. Q. Yongxiang Wang, «Microstructure and wear properties of nitrided AlCoCrFeNi high-entropy alloy,» *Materials Chemistry and Physics,* vol. 210, pp. 233-239, 2018.

[21] T. H. C. T. C. O. M. S. J.-P. M. D. W. B. ,. K. S. V. &. S. C. Pranab Sarker, «High-entropy high-hardness metal carbides discovered by entropy descriptors,» *Nature Communications,* 26 November 2018.

[22] H. I. o. Mineralogy, «Mindat,» 1993-2022, [Online]. Available: https://www.mindat.org/min-1240.html. [Consultato il giorno 6 9 2022].

7. Acknowledgements

I would like to thank:

- My group leader ***Dr Michael Stuer*** for having explained to me how to live and work in the academic and research world. Always motivating me even when results were not encouraging.
- My supervisor ***Dr Amy Jenelle Knorpp*** for supporting and teaching me every day of these six months with her endless smile.
- ***Dr Jon Bell*** for sharing with me his knowledge of characterization techniques. Always glad to talk about movies.
- ***Dr Luca Artiglia*** for the occasion of working at synchrotron at Paul Sherrer Institute.
- ***Dr Matteo Pavese*** for having followed during this thesis work with his precious suggestions and impressions.
- ***Ing Leone Costi*** for the smart talks of every day and his advice.
- ***Ing Matteo Bevione*** for the support in the laboratory and the help during Covid.